VII

COMPARISON OF BOAT-WAKE AND WIND-WAVE ENERGY BUDGETS

Robert J. Byrne, John D. Boon III,
Rhonda Waller and Deborah Blades

A. Introduction

This chapter presents a comparison between the wind-wave energy at each of the study sites described in Chapter IV for the year of observations (October 1978 thru October 1979), and the wave energy in boat wakes during the summer of 1979. This information was produced as part of the study in order to interpret the seasonal appearance of the shoreline profiles at each of the study sites. A discussion of the association between the wave energy budgets and the fastland response is contained in Chapter IX.

A relatively easy way to compare the potential for shore erosion from boat wakes and wind waves is to compare the wave energies from each source. Wave energy is simply proportional to the square of the wave heights. However, a single value of the magnitude of wave energy within a given hour does not explain how that energy may have been distributed within that hour. For example, a few large waves in an otherwise calm hour would contain the same energy as a greater number of smaller waves during the hour. Even a very small wave of 0.1 foot is capable of moving sand when it breaks on the beach, but its zone of influence on the shoreline profile is small.

A larger wave, say 0.5 foot, has the capacity to move more sand per unit area over a larger area.

For this study, the field measurements were used to construct models of the total energy contained in boat wakes and wind waves. In spite of the fact that information on the individual waves is lost when the boat-wake and wind-wave energy budgets are drawn, the expression of energy provides an index for the capacity of boats and the wind to do work on the shoreline profile.

B. Methods

It is important to realize that the values presented for total wind- and boat-wake energies are estimates. A complete portrayal of the wave energy at each site would have required continuous measurement of the waves at each site which was well beyond the scope of the present study. The principal steps involved in the calculation of the boat-wake energy budget were:

1.) Develop for each site the regression relationship between hourly boating frequency and total boat-wake energy per hour. This relationship allows the simple estimation of hourly wake energy from the hourly boating frequency.

2.) Establish the duration of the boating season. This was assumed to extend from 15 May through 15 September. The data obtained in the boating inventory (Chapter VI) indicated a dramatic decrease in boating after about 20 August. Thus two levels of boating activity were assumed to apply: a high level between 10 June and 20 August, and a lower "transition" level between 15 May - 9 June and between 21 August - 15 September.

3.) Establish the average hourly boating frequency for both weekdays and weekends at each site. This was achieved by separately averaging, at each site, the weekday and weekend hourly boating frequencies observed during the inventory of boating activity. In order to describe the higher levels of activity, the values and the averaging was restricted to those observations between 10 July and 20 August. The transition periods (15 May - 9 June and 21 August -15 September) were assumed to contain one-half the hourly boating frequency described during July and August.

4.) For the purposes of computation, the period of boating activity each day was taken as 8 hours. This is reasonably consistent with the observations that most boating occurred between mid-morning and very late afternoon or early evening.

5.) Following steps (1) through (4), the wave energy due to boat wakes was then calculated on a monthly basis and also for the periods between surveys of the shoreline.

i. Boat Wake Energy Calculations

Analyses from the initial 13-day observation period indicated that the hourly boat wake energy was linearly correlated with hourly boat frequency at each of the five sites (Figures 7.1 to 7.5). When boat traffic was light, the signatures of individual boat passes could be discriminated in the record. In these cases, the hourly boat-wake energy was simply the sum of the energies in individual boat passes during the hour. When the boat traffic was so heavy that it was not possible to discriminate individual boat passes, the wave recorder was turned on for 15 minutes each one-half hour so that battery energy would be conserved, thereby insuring the capability of the instrument to measure waves throughout the day. In these situations, the hourly wave energy was calculated as a

multiple of the wave energy contained within the 15 minute segements. But the frequency of boat passes and other characteristics of each passing boat were still continuously recorded on the log sheets.

The actual energy of a wave is directly proportional to the square of the wave height. The total energy contained in each boat wake reaching the shore was calculated as:

$$E_B = \frac{1}{8}\rho g N H^2_{rms} \qquad 7.1$$

where N = Number of boat waves recorded

H_{rms} = Mean square wave height

$= (\Sigma H^2/N_i)^{1}/2, \quad i=1,2,\ldots,N$

ρg = Specific gravity of water

$= 62.5$ lbs/ft^3

The energy given by equation 7.1 requires an adjustment for background energy due to wind waves if any are present. Wind-wave energy contributions were determined from samples of wind waves taken during the absence of boats approximately at the beginning of each hour. Using equation 7.1 together with the number of wind waves present in the sample, an energy "C_w" is calculated as an estimate of the wind-wave energy contribution during subsequent boat-wake events:

$$C_w = E_w \Delta t_B / \Delta t_w \qquad 7.2$$

where Δt_b = Time duration of recorded boat wave event

Δt_w = Time duration of wind wave sample

The adjusted individual boat-wave energy is therefore $E_B' = E_B - C_w$. If two or more boat-wave trains were encountered at one time, the resultant waves are treated as a single event.

ii. Regression Analysis between Wave Energy and Boating Frequency

For the levels of boating activity and boat-wake energies which were collected at the study sites, a line of best fit to the data collected at each site was calculated using linear regression through the origin (Table 7.1, Figures 7.1 thru 7.5). Regression through the origin is required since boat-wake energy must approach zero as the number of boat passes approaches zero. The model for this regression is:

$$E_H = \beta f_H + \varepsilon \qquad 7.3$$

where E_H = Total boat energy for a given hour

f_H = Frequency of boat passes during the hour

β = Regression coefficient

ε = Deviation from regression

---

opposite: Table 7.1 (top) Results of regression analysis: hourly boat-wake energy as a function of hourly boating frequency.

Figure 7.1 (bottom) Regression curve for boating and wake energy at Site A.

next pages: Figures 7.2 to 7.5 Regression curves for boating and wake energy at Sites B thru E.

Results of Regression Analysis: Hourly Boat Wake Energy as a Function of Hourly Boating Frequency, $\hat{E}_H = b\ f_H$.

Site	Regression Equation	Confidence Interval Estimate on Regression Coefficient	Sample Standard Deviation from Regression, $S_{E \cdot f}$
A	$\hat{E}_H = 4.89\ f_H$	$\pm$ 0.73	3.84
	$\hat{E}_H = 3.24\ f_H$	$\pm$ 0.71	7.47
	$\hat{E}_H = 2.24\ f_H$	$\pm$ 0.46	3.69
B	$\hat{E}_H = 2.82\ f_H$	$\pm$ 0.47	5.98
C	$\hat{E}_H = 15.78\ f_H$	$\pm$ 1.47	22.95
D	$\hat{E}_H = 10.64\ f_H$	$\pm$ 1.14	18.86
E	$\hat{E}_H = 2.27\ f_H$	$\pm$ 0.34	2.95

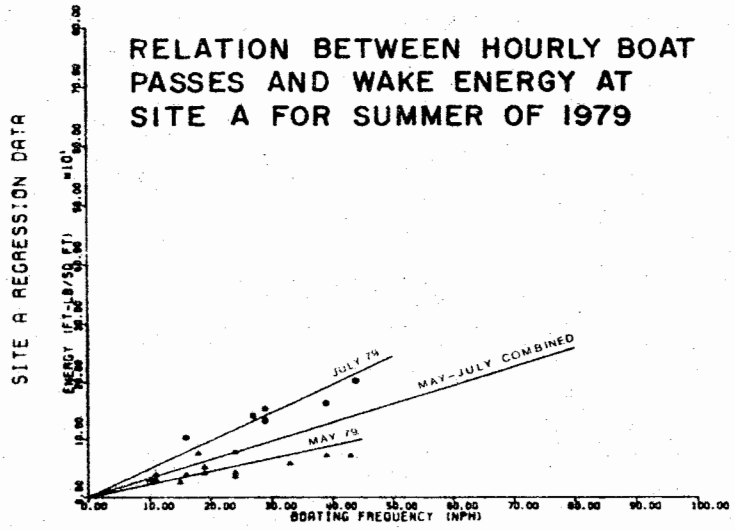

Figure 7.1

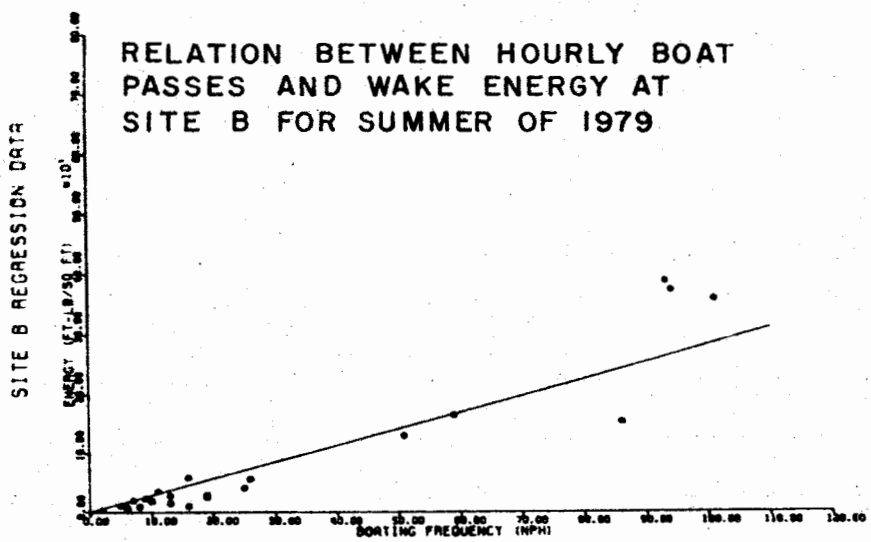

Figure 7.2

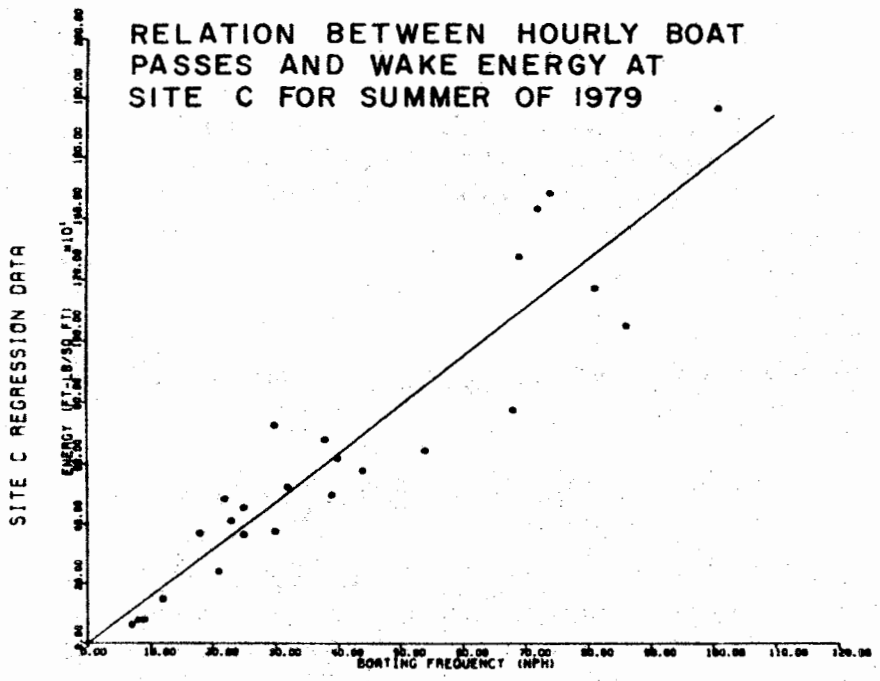

Figure 7.3

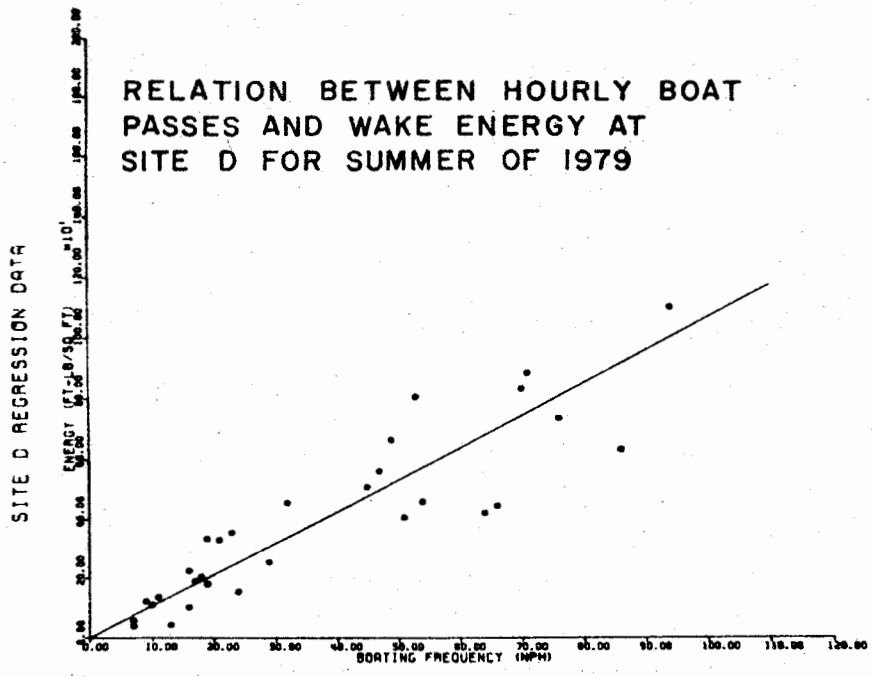

Figure 7.4

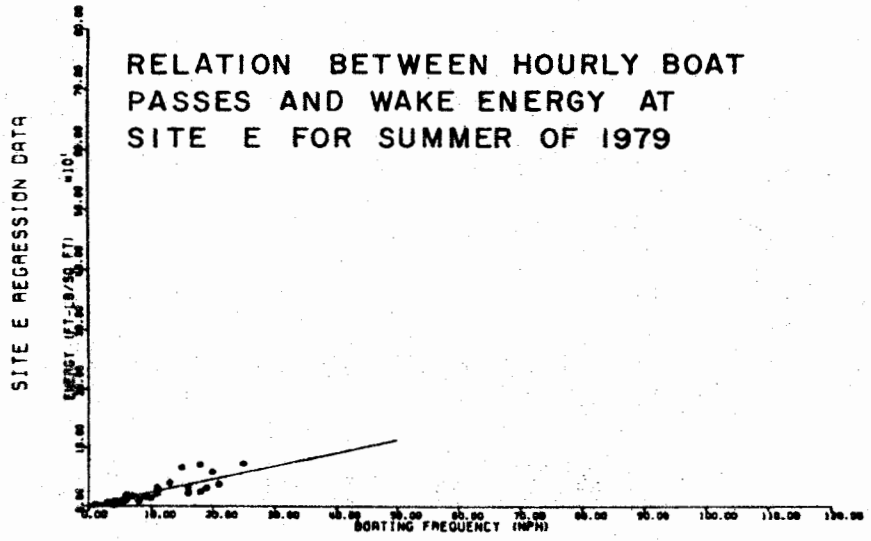

Figure 7.5

For the purposes of this study, an extended form of this model was constructed where the variance of $\mathcal{E}$ is assumed to be directly proportional to the value of f_H. Using the assumption, β is then estimated by the sample regression coefficient "b", which is computed as "b" = $E_H / f_H = \bar{E}_H / \bar{f}_H$.

Obviously, the use of the model for obtaining daily boat-wake energy assumes that the mixtures of boating characteristics remains consistent throughout the boating season, and that the sample data are unbiased. The primary benefit of the model is that it enables the prediction of boat-wake energy to extend to all days during which the fundamental variable of boating frequency had been measured.

Regression analyses were performed for each site using samples from the data acquired throughout the boating season. The results of the regression analyses are presented in Table 7.1 and shown in Figures 7.1 through 7.5. Table 7.1 contains the indiviudal regression estimates for each site, the sample standard deviation from regression ($S_{E \cdot f}$), and a confidence interval estimate on the regression coefficient ($S_b \, t_{.05}$) using Student's "t" at an alpha level of 0.05.

Multiple regression equations were developed for Site A since this site was exposed to wave energies arising from boat traffic using both Harness Creek and South River. Table 6.2 indicates that on weekends approximately 65% of the passes were associated with South River traffic, but the

level dropped to 46% on weekdays. The three regression lines described in Figure 7.1 (and Table 7.1) represent conditions reflecting the different proportions of traffic on South River. The upper curve (July '79) was derived from data samples on the 6th, 11th and 31st of July when only about 25% of the passes were in South River, and thus reflects the energies derived from boats relatively close to shore. The lowest regression line (May '79) represents sample from two days in late May when the majority of boat passes were in the South River and the resulting wave energies reaching the site were relatively small. In the calculation of total boating energy during the boating season (which will be discussed shortly) the regression relation $E_H = 2.24\ f_H$ was used for weekend days and the "combined" regression (Figure 7.6) was used to approximate the relationship for weekdays.

iii. Average Hourly Boating Frequency and Wave Energy Due to Boats

The regression analyses discussed above enable the hourly boat-wave energy to be estimated from the hourly boating frequency At each site, a number of weekdays and weekend days were inventoried during the boating season (Table 6.1). For each of these days an average hourly boating frequency was calculated (Table 6.1 and Figure 7.6). Examination of Figure 7.6 shows that during the latter part of August and during September the average hourly frequency

had diminished relative to the mid-summer period. Although there are fewer observation days in late May and early June, there is also a suggestion that the average hourly frequencies were also less in this early part of the boating season. These periods of diminished activity can be predicted since the local schools recess for summer in early June and return in late August.

For the purpose of estimating the average hourly "mid-summer" boating frequency at each site, the period between 10 June and 20 August was used. The weekday and weekend hourly boating frequencies were separately averaged. It was then assumed that the "transition" periods were characterized by one-half of the respective "mid-summer" levels.

The boating season was assumed to start on 15 May and to end 15 September. Thus the transition periods were 15 May-to-9 June and 21 August-to-15 September. The average hourly boating frequencies so derived are listed in Table 7.2.

The total wave energy in any monthly period (or profile period) is estimated by the hourly wave energy at each site

---

opposite: Figure 7.6 Graph of average hourly boating frequencies at the five study sites.

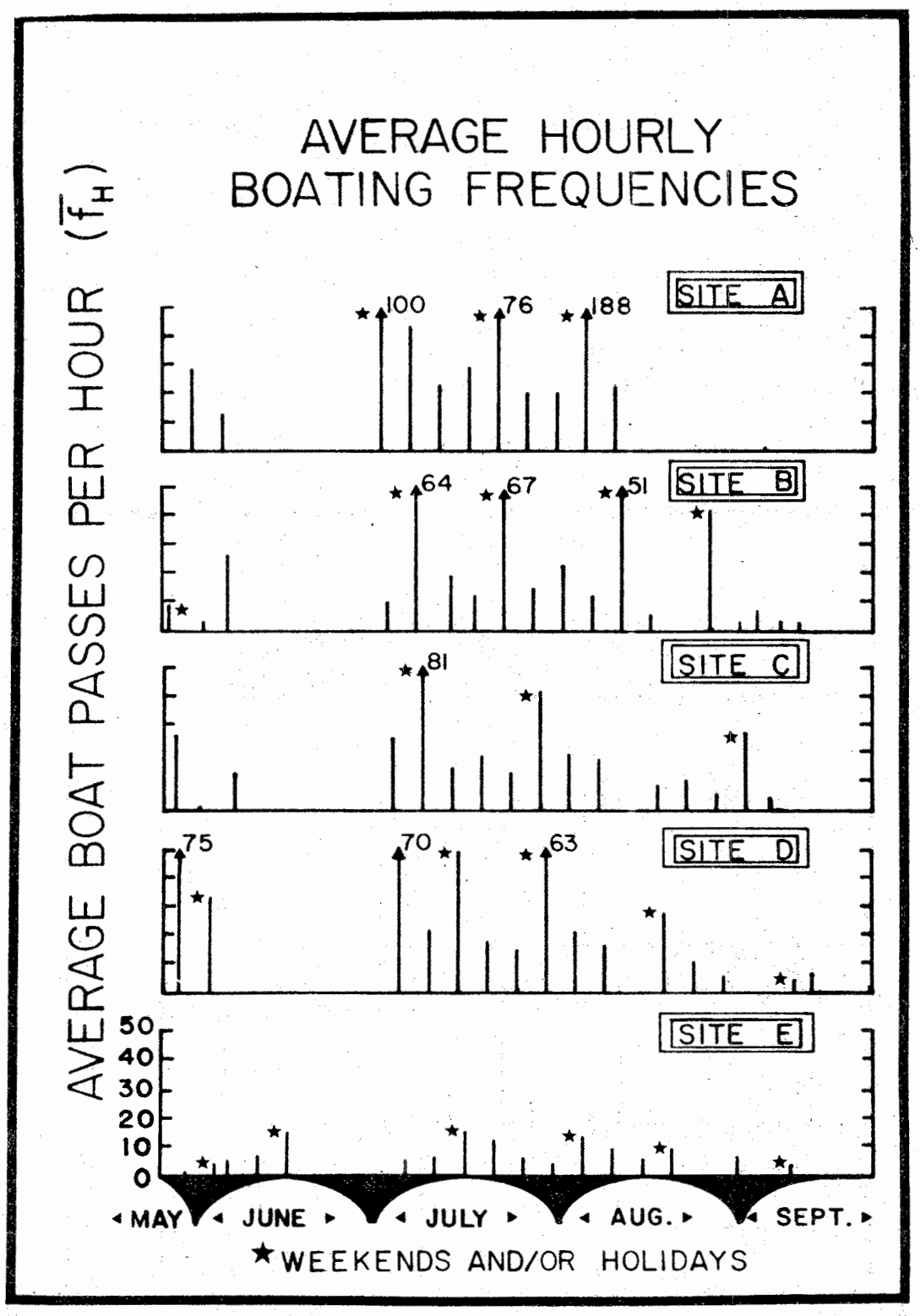
AVERAGE HOURLY
BOATING FREQUENCIES
AVERAGE BOAT PASSES PER HOUR ($\bar{f}_H$)
SITE A
100
76
188
SITE B
64
67
51
SITE C
81
SITE D
75
70
63
SITE E
50
40
30
20
10
0
MAY
JUNE
JULY
AUG.
SEPT.
★ WEEKENDS AND/OR HOLIDAYS

Figure 7.6

TABLE 7.2 Comparison of Wave Energies for Year and Boating Season

YEARLY SUMMARY					BOATING SEASON					
Site	Rank Wind Wave	Wind Wave Energy ($ft\text{-}lbs/ft^2$)	Boat Wake Energy ($ft\text{-}lbs/ft^2$)	Percent Boat Wave Energy	Rank Wind Wave	*Wind Wave Energy ($ft\text{-}lbs/ft^2$)	Boat Wave Energy ($ft\text{-}lbs/ft^2$)	Rank Boat Wave	Percent Boat Wave Energy	% Wind Wave in Boating Season
A	2	5,450,816	118,100	2.2 (1)	2	2,651,077	118,100	3	4.4 (2)	49 (3)
B	3	4,133,173	70,680	1.7	3	1,938,797	70,680	4	3.6	47
C	4	3,823,991	376,040	9.6	4	1,847,511	376,040	1	20.4	48
D	1	6,969,310	247,660	3.6	1	2,948,847	247,660	2	8.4	42
E	5	3,181,249	15,650	0.5	5	1,756,115	15,650	5	0.9	55

*Summed for entire months of May through September, 1979

(1) Percent Boat Wave Energy = (Boat Wake Energy ÷ year total wind wave energy) x 100

(2) Percent boat wave energy = (boat wake energy ÷ boat season wind wave energy) x 100

(3) Percent wind wave in boating season = (wind wave in boating season ÷ year total wind wave energy) x 100

multiplied by the number of days (weekdays and weekend days) and by the number of boating hours per day (which was assumed to be 8 hours).

C. Results

The values for wave energy from wind waves and boat wakes for the year and for the boating season are shown in Table 7.2, together with the relative magnitudes. With respect to wind-wave activity, the sites rank (in decreasing order) D, A, B, C, E for both the total year, and the 1979 "boating season". The sites range C, D, A, B, E with respect to boat-wake energy.

Site C exhibited the highest (20.4%) percentage of boat wake energy during the boating season. Note that Figure 7.7 shows boats were not the principal source of wave energy at any of the shoreline sites during the summer months. Nearly one-half (42-55%) of the total annual wind wave energy occurred during the boating season (May-September).

Monthly summaries of the wind- and boat-wave energies are given in Table 7.3 and Figure 7.7. A summary between

---

opposite: Table 7.2 Comparison of Wave Energies for the Year and Boating Season.

next pages Table 7.3 Wind-wave and boat-wake energy budgets at each site between profile periods.

Table 7.4 (left) Wind-wave and boat-wake energy budgets at each site by month.

Table 7.3 Wind-Wave and Boat-Wake Energy, ft-lbs/ft^2 by Profile Period

Period	SITE A	B	C	D	E
10/29/78-11/25/78	357,845	361,120	241,211	390,062	227,638
11/25/78-12/20/78	397,659	292,156	223,281	409,392	172,665
12/20/78-2/3/79	501,347	388,154	350,278	1,069,687	219,930
2/3/79-3/10/79	36,737	25,469	244,837	512,135	28,905
3/10/79-4/15/79	637,492	526,448	383,118	690,178	334,576
4/15/79-5/25/79	571,142	460,157	435,388	651,301	381,474
5/25/79-6/23/79	529,469	297,318	348,538	556,232	297,539
Boat	43,080	14,160	83,850	56,240	3,560
%	8.1	4.8	24.1	10.1	1.1
6/23/79-7/28/79	538,453	400,853	374,921	610,303	347,469
Boat	56,260	23,240	137,080	90,750	5,720
%	10.4	5.8	36.6	14.9	1.6
7/28/79-8/18/79	369,195	310,968	236,258	408,779	220,484
Boat	32,030	13,300	78,880	53,280	3,370
%	8.7	4.3	33.4	13.0	1.5
8/18/79-9/15/79	578,233	426,361	411,982	670,357	437,187
Boat	17,820	9,400	65,400	36,500	2,300
%	3.1	2.2	15.9	5.4	0.5
9/15/79-10/20/79	721,058	518,193	451,789	770,309	422,181

% Boat Energy = Boat Energy ÷ Wind Wave Energy x 100

Table 7.4 Wind-Wave and Boat-Wake Energy, $ft\text{-}lbs/ft^2$; by Month

Month	SITE A	B	C	D	E
Nov,'78	368,876	382,030	243,274	401,653	231,533
Dec,'78	568,327	397,942	302,422	580,851	232,657
Jan,'79	286,499	220,384	203,256	729,965	131,259
Feb,'79	0	0	241,940	459,637	0
Mar,'79	426,045	290,674	284,571	582,364	240,740
Apr,'79	449,694	436,867	282,900	501,979	244,569
May,'79	494,260	333,635	373,589	550,673	327,697
*Boat	9,200	4,750	28,450	19,740	1,250
% Boat	1.9	1.4	7.6	3.6	.04
June,'79	525,098	297,350	367,197	572,675	320,864
Boat	31,200	25,170	96,980	65,120	4,110
% Boat	5.9	8.5	26.4	11.4	1.3
July,'79	453,541	377,932	303,306	512,831	286,220
Boat	37,700	19,790	117,250	78,940	4,990
% Boat	8.3	5.2	38.7	15.4	1.7
Aug,'79	591,475	443,806	407,363	663,395	397,749
Boat	30,300	15,840	94,180	64,130	4,060
% Boat	5.1	3.6	23.1	9.7	1.0
Sep,'79	586,703	486,024	396,056	649,273	423,585
**Boat	9,700	5,130	30,180	19,730	1,240
% Boat	1.6	1.0	7.6	3.0	0.3
Oct,'79	697,298	466,529	418,117	764,014	344,376

* Boating Energy Based on 15 May - 31 May

** Boating Energy Based on 1 Sept. - 15 Sept.

% Boat Energy = Boat Energy ÷ Wind Wave Energy x 100

profile periods is given in Table 7.2. The zero entries for wave energy at Sites A, B, and E during February, 1979 represent ice-bound conditions. A relatively strong contribution from boat-wake energy at Site C is shown in Figure 7.7. In July 1979, boat-wake energy was 38.7% of the wind-wave energy (27.9% of the total wave energy (Figure 7.7).

It is of interest to compare Sites B and C. Both sites were subject to essentially the same levels of wind energies with the same percentage of that activity occurring during the boating season (47-48%). Inspection of Table 6.2 indicates the two sites have very similar levels of boating activity and about the same ratios of planning versus displacement hulls. Site C had a somewhat higher percentage of water-skiing activity (45% versus 60%). The major difference in the boating activity at the two sites was the distance of the boat passes relative to the shore. At Site B about 80% of the boat passes were at distances

---

next page: Figure 7.7 Histograms of monthly wave energy. Open boxes represent wind-wave energy and blocked boxes represent boat-wake energy. The values entered above the boat-wake energy represent the fraction of boat-wake energy relative to the total (wind plus boat) energy for the month.

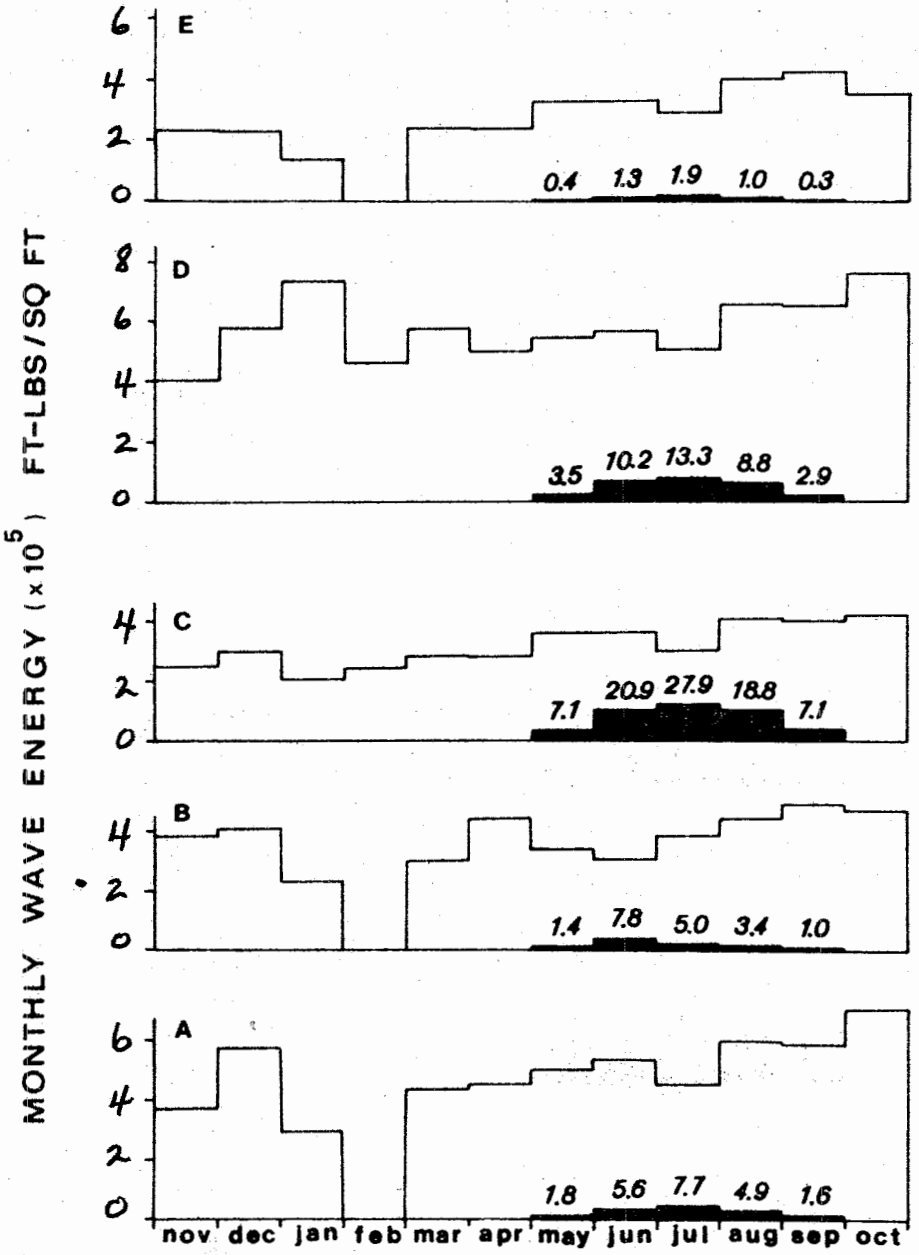
MONTHLY WAVE ENERGY (x10^5) FT-LBS/SQ FT
E
0.4 1.3 1.9 1.0 0.3
D
3.5 10.2 13.3 8.8 2.9
C
7.1 20.9 27.9 18.8 7.1
B
1.4 7.8 5.0 3.4 1.0
A
1.8 5.6 7.7 4.9 1.6
nov dec jan feb mar apr may jun jul aug sep oct

Figure 7.7

greater than 500 feet whereas at Site C over 80% of the boat passes were at distances less than 200 feet. It thus appears that the close proximity of passage at Site C is the principal cause of the relatively high boat-wake energies. In addition, the steeper nearshore bottom gradient at Site C results in less frictional influence on the incoming waves.

VIII

WAVES GENERATED BY PASSAGE OF A BOAT

Robert J. Byrne, John D. Boon III,
Rhonda Waller, and Deborah Blades

A. Introduction

This chapter presents the results of a modest experiment conducted at one of the study sites to understand the behavior of wakes produced by boats cruising at different speeds and distances from the shoreline.

As a boat passes over the water's surface, part of the energy transmitted by the craft's propulsion unit is taken up by the water in the form of surface waves. Thus, the wakes are a manifestation of the resistance offered by the still water to the deformation caused by the boat's hull. The earliest studies of the waves caused by ships were conducted from the viewpoint of how waves effect the resistance of a ship (Froude, 1881; Kelvin, 1887). More recently, attention has been devoted to the relation between ship waves and the stability of banks on the waterways through which the boats pass (Johnson, 1957; Das, 1969; Sorenson, 1967).

The pattern of waves in a boat wake depends partially on the value of the Froude number "F"* (which is the ratio

---

*The Froude Number is not directly measurable, but represents the ratio of two variables which often become "lumped together" in theoretical wave-energy equations. The Froude Number "F" is the ratio of the boat speed "V_s" and the speed "C" of a wave in shallow water. The wave speed is in turn a function of the basin depth "d", since $C = \sqrt{gd}$. ("g" is the acceleration due to gravity; "g" = 32 feet/sec.^{2}). So... Froude Number "F" = $V_s / \sqrt{gd}$.

between the boat speed "V_s", and the speed "C" of a wave in shallow water). Both the Froude number and the configuration of a boat hull influence the maximum wave height which will be experienced at a given distance from the sailing line of the boat.

A displacement hull will generate a series of waves at the bow and stern (Figure 8.1). At values of "F" below 1, the wave pattern in the vicinity of the boat, together with the maximum wave height, can change fairly dramatically as the wake travels away from the boat. Each set of waves produced at the bow and stern include a series of waves diverging from the sailing line and a series of transverse waves which move in the direction of boat passage. The intersections of the transverse and diverging waves are points of higher wave heights where breaking waves are most likely to occur in the wake.

These "cusp" locations may be connected to form a locus of cusps which define an angle "$\emptyset$" which the wave front makes with the sailing line (Figure 8.1). The theoretical development of Kelvin (1887) predicts a value of $\emptyset$ = 19°28' for Froude number values less than 0.7 and for values greater than about 3. However, for intermediate "F" values, the angle "$\emptyset$" approaches a maximum of 90° when "F"=1. At this point the transverse and diverging waves combine to

---

opposite: Figure 8.1 (top) Schematic drawing of waves generated by moving boat.

Figure 8.2 (bottom) Definition sketch of boat wake packet.

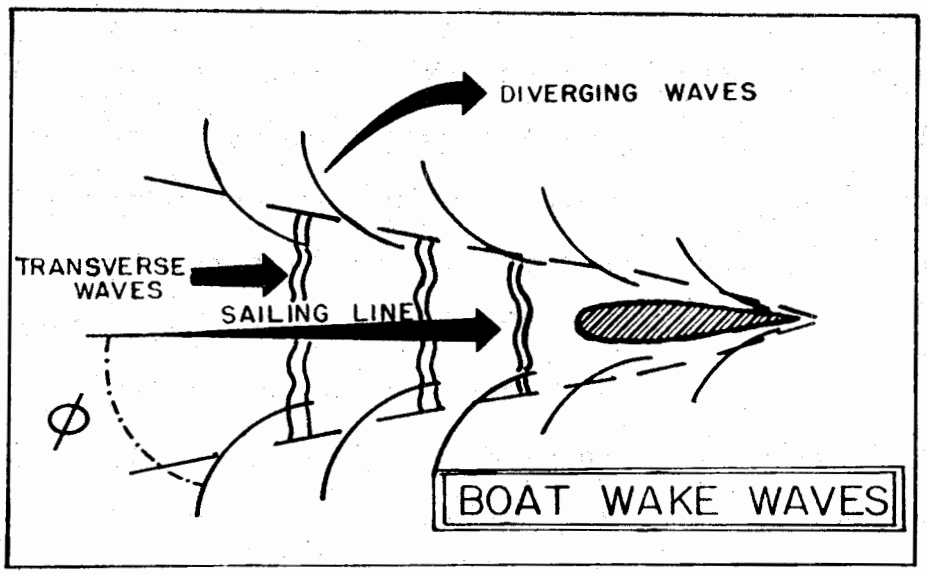

Figure 8.1

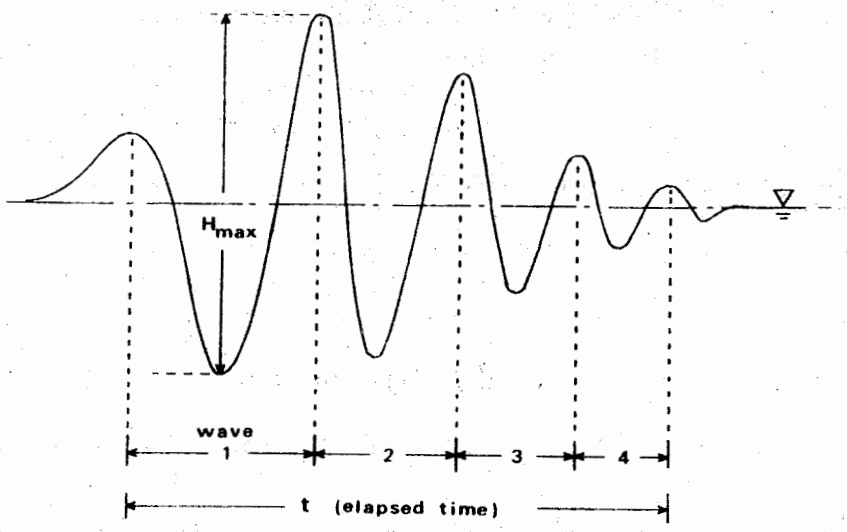

Figure 8.2

form a single wave with its crest normal to the sailing line.

Besides the angle $\emptyset$, the maximum wave height (and thus total energy) in the wake wave "packet" varies with the Froude number. A typical boat-wake wave packet is shown schematically in Figure 8.2. Within the packet there is a single wave with maximum height. Results of some experiments with boat models in a towing tank (Johnson, 1957) are shown in Figure 8.3 to illustrate the nonlinear behavior of "H_{max}" with Froude number "F". After passing the critical value of "F", the values of "H_{max}" tend to approach a constant value.

B. Field Measurements of Controlled Boat Passes

The experiment was conducted at Site C (Broad Creek), using boats operated by the Maryland Department of Natural Resources Marine Police. Two boats were used: a 26 ft. Uniflite cruiser (Marine Police boat "Somerset"), and a 16 ft. Boston Whaler. The Uniflite is a deep-V planing hull while the Boston Whaler is a 3-point planing hull. Replicate passes were made at distances of 200, 150, and 100 ft. (also 50 ft. in the case of the Whaler) from the shoreline for a range of speeds between 6 and 30

---

opposite: Figure 8.3 (top) Maximum wave height as a function of Froude Number for typical ship model (Johnson, 1957).

Figure 8.4 (bottom) Typical record of boat wake passing the wave gage in shallow water.

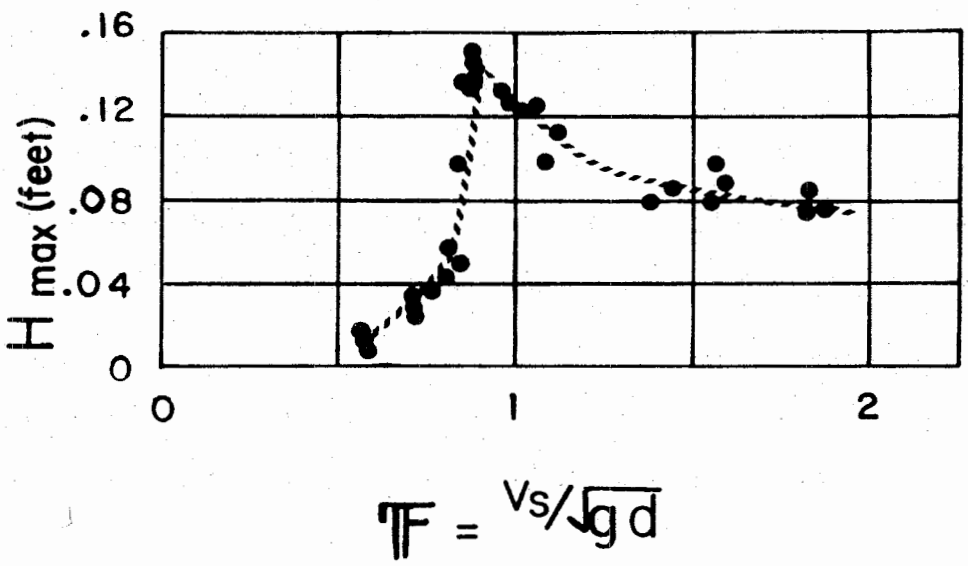

Figure 8.3

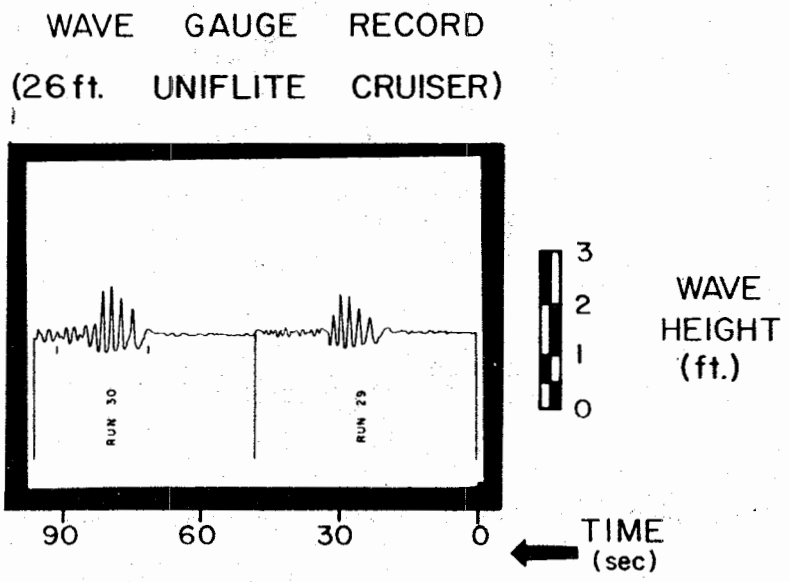

Figure 8.4

knots. Boat speed was determined by measuring the time for the boat to travel between two buoys anchored 100 ft. apart. The surface wave gauge (described in Appendix A) was located approximately 24 feet from the shoreline in a water depth of about 2.2 feet. With very rare exception none of the waves in the generated trains broke seaward of the wave gauge position. A typical wave record produced during the trial runs is shown in Figure 8.4.

The results of the experiment are shown in Tables 8.1 and 8.2. In these calculations several different parameters are of interest. These are:

"H_{max}" = the highest wave of the group (measured in feet).

"$\bar{T}$" = the average wave period (defined as the number of waves divided into the duration of the wave packet).

"$\bar{E}$" = average energy per unit surface area ($ft\text{-}lbs/ft^2$)

$= \frac{1}{8} \rho g H_{rms}^2$, where "$H_{rms}$" $= (\Sigma H^2/N_i)^{1/2}$

$i = 1,2,\ldots,N$

"E_T" = total energy in wave train ($ft\text{-}lbs/ft^2$)

$= \frac{1}{8} \rho g N H^2_{rms}$

"F" $= 1.667\ V_s/\sqrt{gd}$ for boat speed in knots.

The results of the trial runs are graphed in Figures 8.5 thru 8.12. In the plot of "F" versus "H_{max}" (Figures 8.5 and 8.6), there is an apparent peak in "H_{max}" at values of "F" between 0.8 to 1.0. A definite relation of "H_{max}" to the distance of the boat from the shore is also

apparent, and this relationship is stronger for the deep-V hull. Figures 8.7 and 8.8, which are of boat speed versus "H_{max}", offer a simpler illustration of how "H_{max}" varies with different boat speeds. As expected, the deep-V hull of the 26 ft. cruiser generated the larger waves. The largest "H_{max}" occurred for speeds between 8 and 10 knots when the cruiser was in the displacement mode, and the "H_{max}" values ranged between 1.25 and 1.75 ft. for the distances tested. These values far exceed those which were expected for wind-generated waves.

It is of interest to note that the dependence of "H_{max}" (or energy, Table 8.1) upon boat speed is highly nonlinear. For the circumstances tested, "H_{max}" varies in a nonlinear fashion with the inverse of speed. The "H_{max}" for the Uniflite cruiser decreased as the boat speed was increased beyond a "critical" value of 8 to 10 knots. In the case of the 16 ft. planing hull of the Boston Whaler, the "critical" speed occurred between 6 and 8 knots when the Whaler was in the displacement mode.

For distances of 100 to 200 ft. from the shoreline, the data in Figure 8.5 show there is little dependence for either the Whaler or the Uniflite Cruiser between "H_{max}" and the distance of the boat from shore. However, at the closer boat passes of 50 ft., the range of "H_{max}" is dramatically increased. Again the nonlinear dependence of

---

next pages: Tables 8.1 and 8.2 Summary of observations of controlled boat passes.

Table 8.1 Summary of Observations: 26 ft. Uniflight Cruiser

Run	Speed MPH	Speed Knots	Distance (ft.)	Number of Waves	H_m (ft.)	$\overline{E}$ (ft-lb/ft^2)	E_T (ft-lb/ft^2)	Duration t (sec)	$\overline{T}$ (sec)	F (V in knots
11	28.4	24.9	200*	15	0.58	1.09	16.35	34.2	2.3	2.04
12	31.0	27.3	200	15	0.58	1.08	16.20	33.0	2.2	2.23
13	23.5	20.7	200	17	0.74	1.36	23.12	39.0	2.3	1.69
14	20.0	17.6	200	19	0.85	1.41	26.79	41.1	2.2	1.44
15	8.6	7.6	200	15	1.30	2.75	41.25	38.1	2.5	0.62
16	10.2	9.0	200	15	1.81	4.71	70.65	45.0	3.0	0.74
17	6.3	5.5	200	17	0.56	0.48	8.16	28.2	1.7	0.45
18	6.5	5.7	200	17	0.71	0.53	9.01	24.3	1.4	0.47
19	32.5	28.6	150	17	0.67	1.06	18.02	37.8	2.2	2.43
20	31.0	27.3	150	17	0.69	1.09	18.53	33.9	2.0	2.32
21**	20.7	18.2	150	9	1.12	4.08	36.72	21.6	2.4	1.55
22**	20.7	18.2	150	11	0.96	2.99	32.89	25.2	2.3	1.55
23**	9.6	8.4	150	11	1.58	4.64	51.04	30.0	2.7	0.71
24	13.6	12.0	150	9	0.98	4.25	38.25	22.2	2.5	1.02
25	11.8	10.4	150	9	1.23	6.04	54.36	26.4	2.9	0.88
26	6.4	5.6	150	6	0.60	1.13	6.78	9.0	1.5	0.48
27	6.8	6.0	150	6	0.71	1.37	8.22	9.3	1.6	0.51
28	29.6	26.0	100	6	1.03	3.76	22.56	12.9	2.2	2.42
29	29.6	26.0	100	6	0.96	3.53	21.18	14.1	2.4	2.42
30	22.0	19.4	100	9	1.14	3.81	34.29	19.8	2.2	1.81
31	20.0	17.6	100	9	1.07	3.18	28.62	18.0	2.0	1.64
32	11.0	9.7	100	6	1.36	7.50	45.00	18.3	3.1	0.90
33	11.8	10.4	100	6	1.34	7.08	42.48	19.8	3.3	0.97
34	6.6	5.8	100	9	0.71	1.05	9.45	14.7	1.6	0.54
35	6.9	6.1	100	9	0.74	1.26	11.34	18.6	2.1	0.57

** Largest wave broke just seaward of wave gage

* Water depth at 200 ft = 13 ft.
150 ft = 12 ft.
100 ft = 10 ft.
50 ft = 3 ft.

Table 8.2 Summary of Observations: 16 ft. Boston Whaler

Run	Speed MPH	Speed Knots	Distance (ft.)	Number of Waves	H_m (ft.)	$\overline{E}$ (ft-lb/ft^2)	E_T (ft-lb/ft^2)	Duration t (sec)	$\overline{T}$ (sec)	F (V in knots)
1	28.4	25.0	200	28	.179	0.11	3.08	46.8	1.7	2.04
2	32.5	28.6	200	29	.201	0.11	3.19	48.0	1.7	2.34
3	20.7	18.2	200	21	.290	0.25	5.25	36.3	1.7	1.49
4	26.2	23.0	200	25	.290	0.23	5.75	42.6	1.7	1.88
5	9.6	8.4	200	22	.335	0.38	8.36	40.2	1.8	0.69
6	11.8	10.4	200	22	.446	0.49	10.78	45.6	2.1	0.85
7	6.5	5.7	200	15	.312	0.30	4.50	24.3	1.6	0.47
8	6.9	6.1	200	19	.290	0.26	4.94	30.0	1.6	0.50
9	31.0	27.3	150	22	.246	0.15	3.30	33.9	1.5	2.32
10	31.0	27.3	150	22	.223	0.16	3.52	34.5	1.7	2.32
11	20.7	18.2	150	16	.335	0.34	5.44	27.6	1.7	1.55
12	22.0	19.4	150	17	.312	0.29	4.93	31.2	1.8	1.65
13	13.4	11.8	150	15	.468	0.55	8.25	30.9	2.1	1.00
14	9.6	8.4	150	14	.402	0.66	9.24	27.9	2.0	0.71
15	6.2	5.4	150	10	.357	0.37	3.70	17.4	1.7	0.46
16	6.5	5.7	150	10	.469	0.56	5.60	14.1	1.4	0.48
17	34.1	30.0	100	12	.312	0.31	3.72	19.8	1.7	2.79
18	32.5	28.6	100	16	.268	0.20	3.20	21.9	1.4	2.66
19	20.7	18.2	100	10	.402	0.54	5.40	17.7	1.8	1.70
20	23.5	20.7	100	11	.357	0.40	4.40	18.3	1.7	1.93
21	10.2	9.0	100	10	.513	1.00	10.00	19.5	2.0	0.84
22	11.4	10.0	100	10	.491	0.87	8.70	16.2	1.6	0.93
23	6.2	5.5	100	11	.469	0.41	4.51	20.5	1.9	0.51
24	7.9	7.0	100	10	.670	1.10	11.00	17.7	1.8	0.65
25	32.5	28.6	50	4	.491	0.80	3.20	6.0	1.5	4.86
26	17.9	15.8	50	4	.759	1.71	6.84	6.3	1.6	2.69
27	9.7	8.5	50	5	.781	1.45	7.25	9.9	2.2	1.44
28	27.3	24.0	50	5	.446	0.73	3.65	8.4	1.7	4.08
29	17.0	15.0	50	4	.670	1.30	5.20	6.0	1.5	2.55
30	11.4	10.0	50	4	.737	1.44	5.76	7.2	1.8	1.70
31	7.6	6.7	50	13	.893	0.93	12.09	31.5	2.4	1.13
32	7.2	6.3	50	14	.759	0.90	12.60	30.6	2.2	1.07
33*	23.5	20.7	200	19	.312	0.26	4.94	29.7	1.6	1.69
34*	27.2	23.9	150	16	.357	0.34	5.44	30.6	1.9	2.03
35*	27.2	23.9	50	15	.402	0.52	7.80	23.4	1.6	4.06

*with water skier

"H_{max}" and distance is shown, although "H_{max}" for the Whaler approaches a constant value beyond the "critical" speed more quickly than in the case of the deep-V hull. This is no doubt due to the fact that the planing mode is achieved at lower speeds in the Boston Whaler than in the Uniflite Cruiser.

Since the principal concern of this study is the magnitude of energy reaching the shoreline with each boat pass, plots of total wave energy "E" in the respective wave packets is shown as a function of the Froude Number "F" (with distance as a parameter) in Figures 8.9 and 8.10. The results presented above show there is a strong nonlinear relationship between "F" and "H_{max}", so it is not surprising that a similar nonlinear relationship exists between "F" and total wave packet energy at the shoreline. In the case of the deep-V hull (26 ft. Uniflite cruiser) there is only a slight suggestion that wake energy is dependent upon the distance from the shore for any given speed. In the case of the Whaler, only those boat passes at the 50 ft. distance show clear separation in their wake energies. Part of the reason for a reduction in wave energy from boats passing at greater distances from the shore is that the number of waves in a packet depends upon distance. For example, Tables 8.1 and 8.2 show that waves generated at close distance for any given speed contain higher waves but fewer in number.

It is important to note that the peak values of "E_T" and "H_{max}" in Figures 8.9 and 8.10 lie in vicinity of "F" = 0.8 rather than the theoretical value of "F" = 1. This observation is consistent with the results of similar experiments with the wakes of larger-hulled craft reported by Sorenson (1967).

Three runs were made by the Boston Whaler with a water skier in tow. This condition was tested to see in a preliminary way whether the effects of the skier's weight would cause the planing hull to "squat" and thereby generate larger "E_T" in the wake. The plot of "E_T" versus "F" (Figure 8.9) does not clearly distinguish a difference. However, a plot of "E_T" versus boat speed (Figure 8.11) suggest there may be an effect, since two of the three runs do show values for "E_T" which are higher than the general trend. While these few runs cannot be considered to display a truly significant difference, the results do suggest that the effect of water skiers on boat wakes should be examined further in future tests.

The most important observation to be drawn from these experimental boat runs is that maximum values of

---

next pages: Figures 8.5 (upper left) and 8.6 (lower left) Variation in maximum wave height "H_{max}" as a function of Froude Number with distance of passage as a parameter.

Figures 8.7 (upper right) and 8.8 (lower right) Variation in maximum wave height "H_{max}" as a function of boat speed with distance of passsage as a parameter.

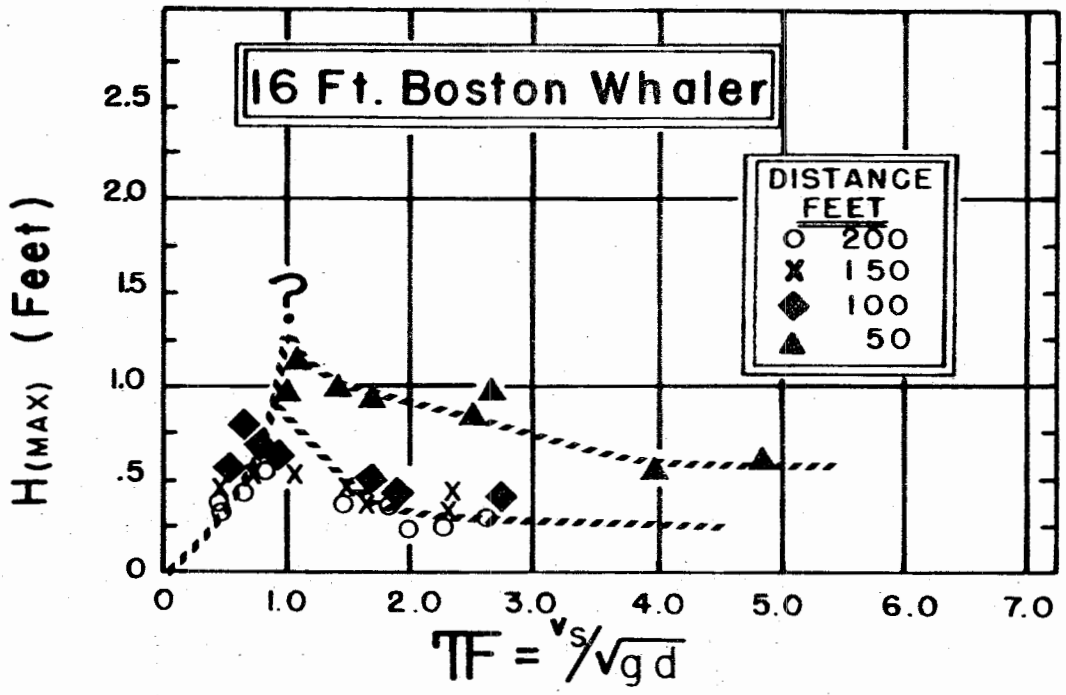

Figure 8.5

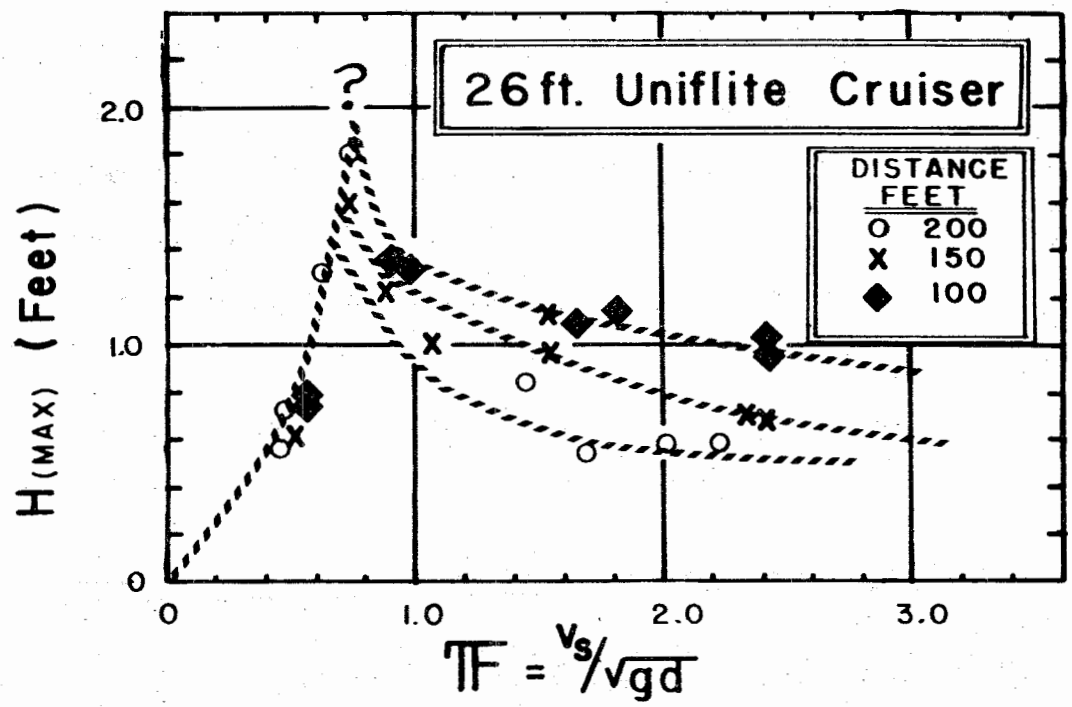

Figure 8.6

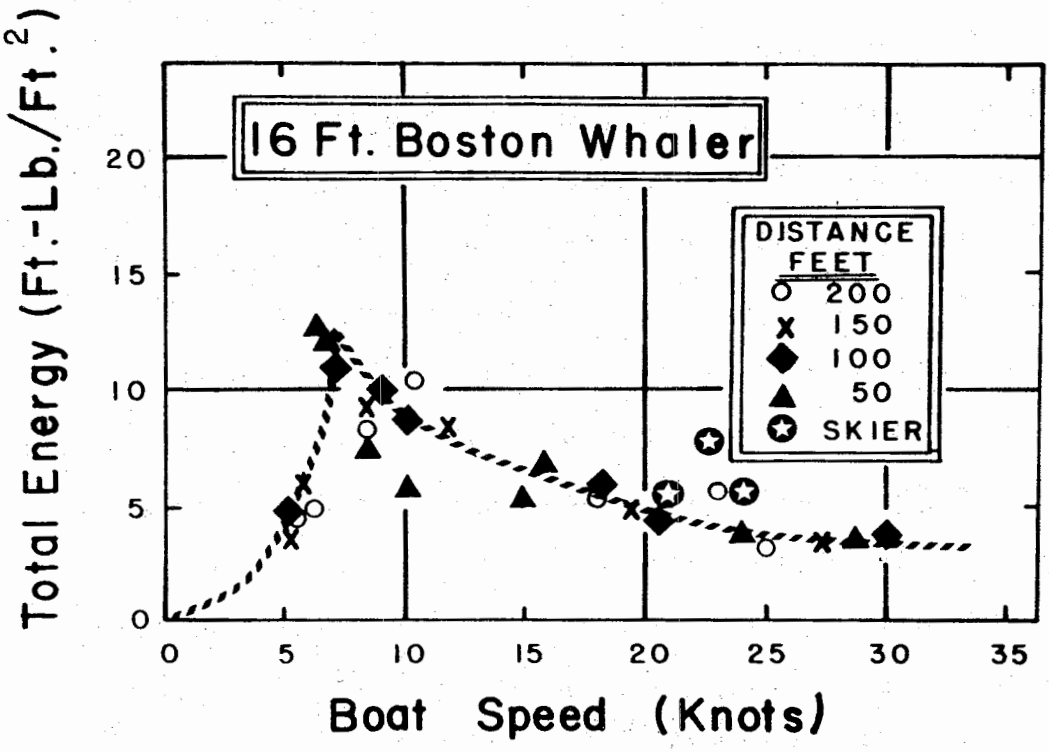

Figure 8.7

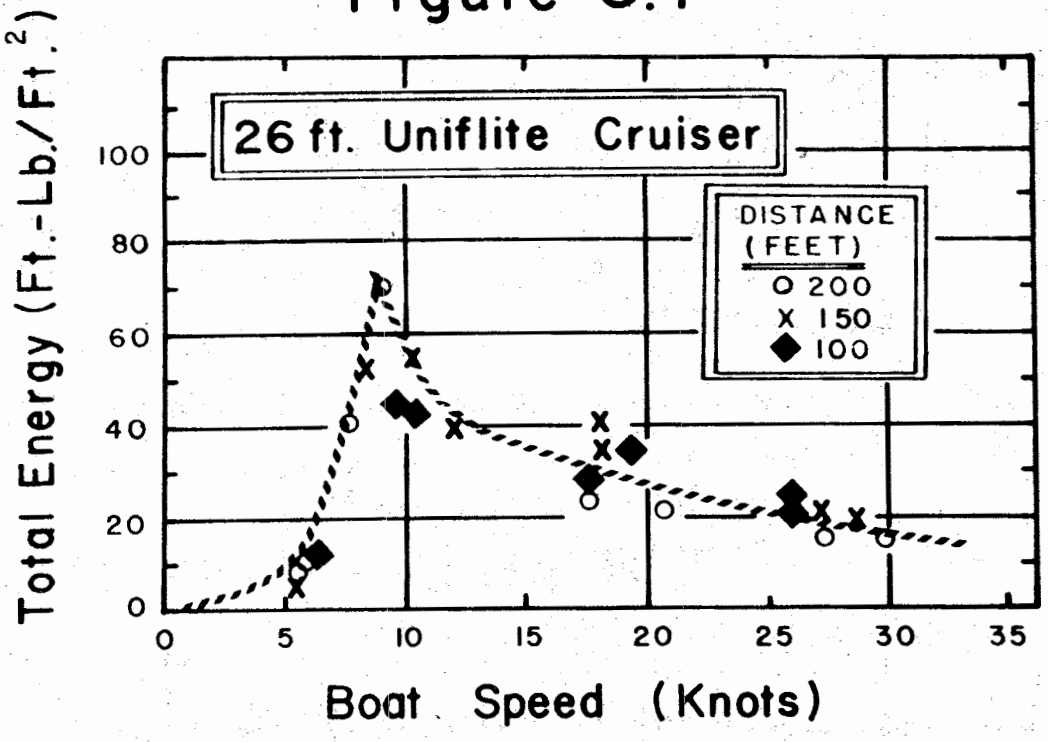

Figure 8.8

wave heights (and wake energy) are generated for Froude numbers in the range between 0.7 and 1.0. Since the Froude number is dependent upon water depth as well as boat speed, those boat speeds which generate maximum wakes will vary with different water depths in different waterways. Table 8.3, which lists the various Froude numbers arising from different combinations of boat speed and water depth, provides a simple illustration of what might be expected for a variety of "typical" conditions. For example, suppose a boat was travelling at a steady speed of 6 knots while running up a creek in which the depth decreased from 18 ft. at the mouth to 4 ft. near the head. During the run the Froude number would be small near the mouth ("F" = 0.42 to 0.56, respectively, for water depths of 18 ft. and 10 feet) and relatively small wave heights would be generated in the wake. But, when the boats reached depths less than 6 feet, the Table shows that maximum wave heights would be generated.

Table 8.3 can also be used to show the effects of another kind of boating pattern. Consider a creek where the water depth varies from 10 feet at the centerline to 2 feet

---

opposite: Table 8.3 Froude number for different combinations of water depth and boat speed.

next pages: Figure 8.9 (upper left) and 8.10 (lower left) Total energy in the wave packet as a function of Froude Number with distance of passage as a parameter.

Figure 8.11 (upper right) and 8.12 (lower right) Total energy in the wave packet as a function of boat speed with distance of passage as a parameter.

TABLE 8.3 FROUDE NUMBER for COMBINATIONS of WATER DEPTH and BOAT SPEED

DEPTH (ft)	SPEED (Knots)								
	2	4	6	8	10	12	14	16	18
2	0.42	0.83	1.25	1.66	2.08	2.49	2.91	3.32	3.74
4	0.29	0.59	0.88	1.17	1.47	1.76	2.06	2.35	2.64
6	0.24	0.48	0.72	0.96	1.20	1.44	1.68	1.92	2.16
8	0.21	0.42	0.62	0.83	1.04	1.25	1.45	1.66	1.87
10	0.18	0.37	0.56	0.74	0.93	1.11	1.30	1.49	1.67
12	0.17	0.34	0.51	0.68	0.85	1.02	1.19	1.36	1.52
14	0.16	0.31	0.47	0.63	0.78	0.94	1.10	1.26	1.41
16	0.15	0.29	0.44	0.59	0.73	0.88	1.03	1.17	1.32
18	0.14	0.28	0.42	0.55	0.69	0.83	0.97	1.11	1.25

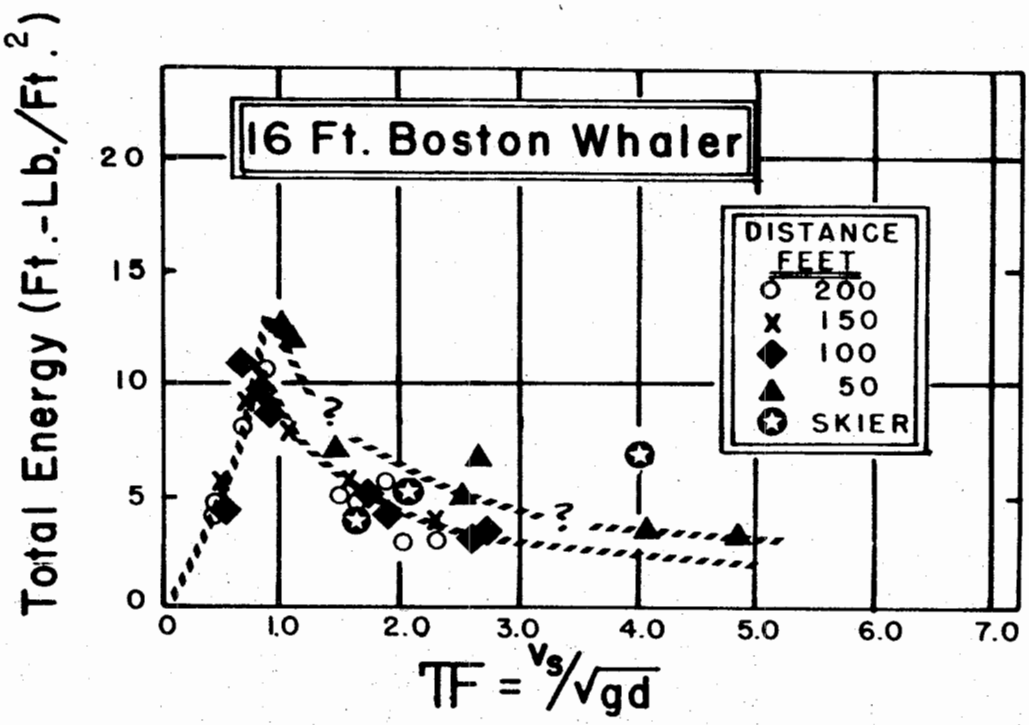

Figure 8.9

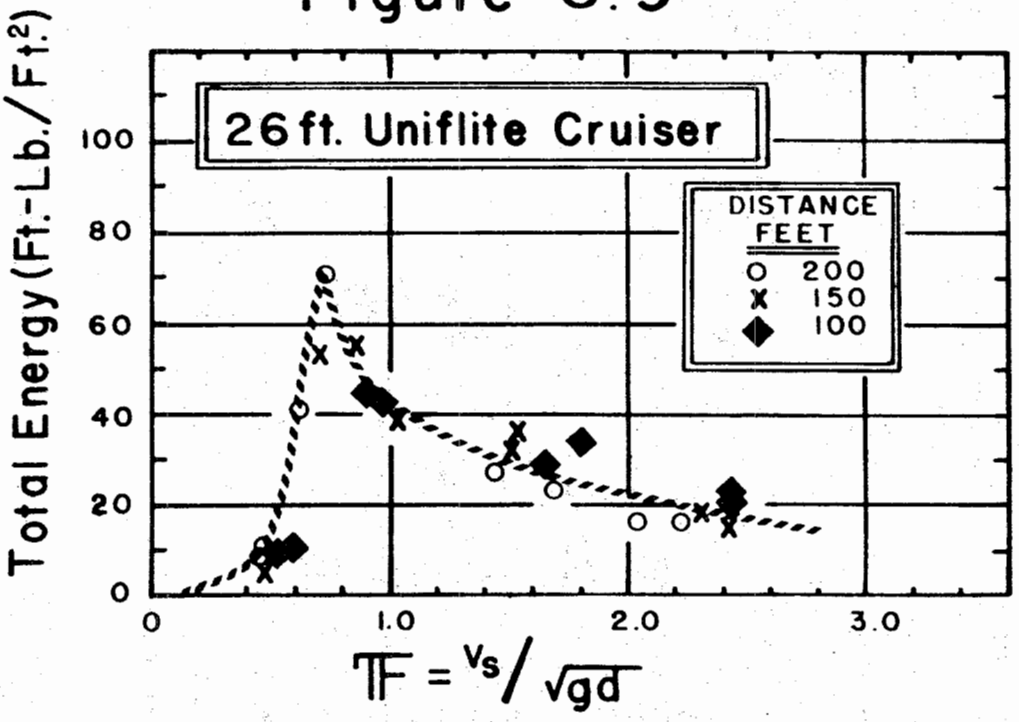

Figure 8.10

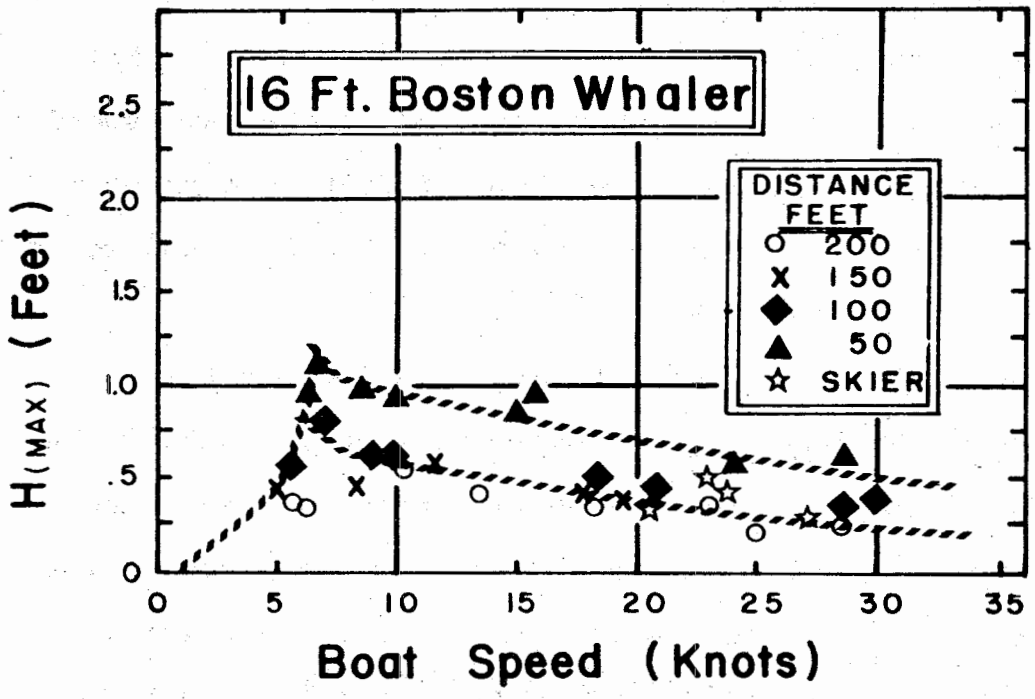

Figure 8.11

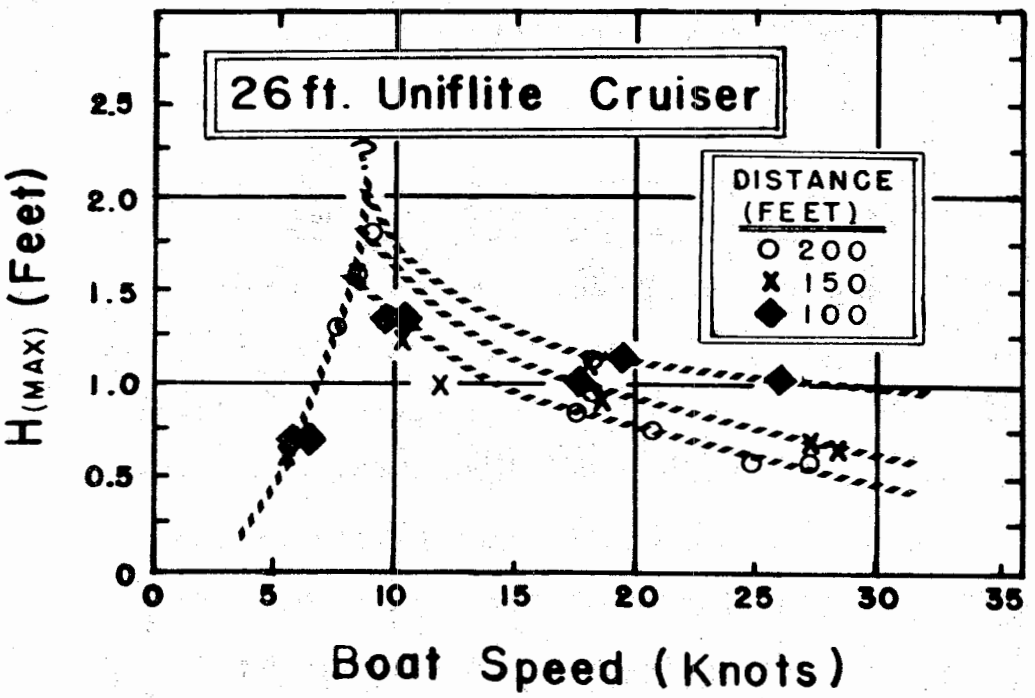

Figure 8.12

near the bank. A boat travelling the centerline at a steady speed of 6 knots would have a low Froude number (0.56) and small wake. The same boat travelling at the same speed closer to the shore in water depths of 6 feet or less would be in the Froude number range between 0.7 and 1.25 and would be generating a maximum wake.

Table 8.3 does not, unfortunately, allow for the prediction of the magnitude of the wave energy reaching the shore. The absolute magnitude of wave energy in any wake would depend upon hull characteristics and the slope of the nearshore bottom, together with the boat speed and water depth where the boat passes any particular shoreline site. But, Table 8.3 shows that distance from shore is important in producing the wake in any specific boat pass.

C. Suspended Sediments Resulting from Boat Wakes

Besides measuring wake characteristics in some trial runs, other data were collected at Site C to give a very preliminary idea of the increase in suspended sediment associated with breaking waves in boat wakes along the shoreline. For this experiment, the Uniflite cruiser travelling at a speed of approximately 21 knots made repeated passes 200 ft. offshore, and samples were taken after the breaking of the 1st, 5th, and 10th wake packets. The water in the nearshore was also sampled prior to the passage of the boat and again at the end of all of the

passes of the Uniflite cruiser. The samples were collected by immersing one-quart jars about 5 cm. under the water surface immediately after the last wave in each packet broke on the shoreline profiles. The water samples were filtered through pre-weighed 0.6 μm Nuclepore filters. After desiccation, the filters were reweighed to determine total weight of suspended sediments. Then the samples were completely combusted to obtain the percent of organic material.

The results are shown in Table 8.4.

Table 8.4. Suspended Sediment Concentrations

Run	Time	Total Concentrations	Percent Organic
1.) Ambient	1045 EDT	0.0053 grams/liter	35.7
2.) 1st Packet	1125	0.440	20.3
3.) 5th Packet	1127	0.120	21.8
4.) 10th Packet	1130	0.330	23.2
5.) End of Passes	1407	0.081	14.3

Due to a relatively high stage of the tide when the Uniflite runs were conducted, breaking waves extended across the entire foreshore, and the swash impinged against the bank scarp at Site C (Figure 4.17). Table 4.4 shows the foreshore sediments at this site are composed principally of sand with only a few percent of silt and clay. Yet, the data in Table 8.4 show that the breaking waves resulted in an enhancement of the short-term load of suspended material by more than two orders of magnitude over the ambient level.